

RESEARCH ARTICLE



ISSN: 2321-7758

MACROSTRUCTURAL ANALYSIS AND APPLICATIONS OF SAMARIUM (Sm^{3+}) DOPED Mn-Cr SPINEL FERRITES PREPARED BY SOL-GEL METHOD

GURRALA ALLURIAH¹, GUDISA KISHORE²

¹Lecturer in Chemistry, S.V Arts and Science College, Giddalur, Prakasam District

²Lecturer in Chemistry, TRR Government Degree College, Kandukur, Prakasam District



ABSTRACT

The effect of Samarium (Sm^{3+}) ion substitution on the structural and magnetic properties of manganese-chromium (Mn-Cr) ferrite of chemical formula $\text{Sm}_x \text{Mn}_{0.3} \text{Cr}_{0.3} \text{Fe}_{2-x} \text{O}_4$ ($x=0.0, 0.2$ and 0.4) has been studied. Samarium substituted nanoferrites synthesised by sol-gel method and annealed at 700°C to improve the structural and magnetic properties. Structural changes of nano ferrites due to the substitution of Samarium ion were identified by X-ray diffraction (XRD), particle sizes of several diffraction and average crystallite size were measured from the XRD data based on Debye-Scherrer' equation. Fourier Transform infra-red spectroscopy FTIR, The morphological analysis of the sample is studied using scanning electron microscopy (SEM), elemental composition studies done by energy dispersive X-ray spectroscopy (EDAX), and average particle diameter identified by Transmission electron microscopy (TEM) studies. FTIR spectral studies of prepared samples under investigations disclose the formation of a single phase spherical particles, showing two important absorption bands one (ν_1) around 556.2 cm^{-1} is recognized to the intrinsic vibrations of tetrahedral complexes and another low frequency band (ν_2) around 431 cm^{-1} is owing to octahedral complexes.

Key Words: Nano ferrites, Sm^{3+} substitution, Structural and magnetic properties

©KY PUBLICATIONS

1.0 Introduction

Ferrites are ferrimagnetic semiconductors that released a new area in the physics of material science and the needful high resistivity ferrites directed to production of various ferrites. Ferrite materials very important materials in the manufacturing of many electromagnetic devices like inductors, isolators, circulators, converters, phase shifters and electromagnetic wave absorbers¹. Spinel ferrites have been studied extensively due to easy to synthesis and abundant uses in technological and industrial applications. Synthesis of Nano ferrites like metallic spinel ferrites, characterized by a low size distribution is important due to their notable electrical and

magnetic properties and wide practical applications in information advanced technologies like, magneto caloric refrigeration, medical diagnostics etc,. Magnetic properties of Nano Ferrite's are affected by the type of the substituent, microstructure, chemical composition, method of preparation, cation distribution in the tetrahedral (A) and octahedral [B] sites, grain size, voids, surface layers, and doping. Electro & Magnetic Nano ferrites with general structure MFe_2O_4 have been successfully synthesized through various methods including sol-gel method, co-precipitation method². There is many attempt have been made in order to improve the qualities of ferrites by including the same suitable

nonmagnetic/diamagnetic contaminations with different valence state at the A and B sites includes Samarium (Sm^{3+}). Manganese ferrites are well known magnetic materials with cubic spinel structure which have been widely used in different technological applications. The properties of these ferrites greatly depend on the composition, size and morphology, which are strongly associated with the preparation conditions³. Till now, various compositions of manganese ferrites prepared, structural and sizes have been synthesized in different methods^{4,5}. Among these techniques, sol-gel method offers high degree of compositional uniformity content in a relatively short processing time at a very low temperature for the synthesis of nano ferrites.

G. Kumar⁶ stated that the rare earth oxides are good electrical insulators having high electrical resistivity; therefore, in spinel ferrites the proper choice of rare earth cation will modify the electrical and magnetic properties. Substituting the parent ferrite with selected rare earth ions leads to different morphological changes. Thus, in this investigation, the effect of Sm^{3+} substitution in $\text{Mn-Cr-Fe}_2\text{O}_4$ is studied. The sol-gel method is used to synthesize the nanoparticles of $\text{Sm}_x\text{Mn}_{0.3}\text{Cr}_{0.3}\text{Fe}_{2-x}$. The structural and magnetic properties of the synthesized samples have been discussed in the contents.

2.0 Experimental

2.1 Material and Method

All chemicals and solvents were AR grade or better purchased from Merck Co. Pvt Ltd and Sd. fine chemical used without any further purification. The stoichiometric amounts of metal nitrates viz., $\text{Sm}(\text{NO}_3)_3 \cdot 6\text{H}_2\text{O}$, Ferric Nitrate [$\text{Fe}(\text{NO}_3)_3 \cdot 9\text{H}_2\text{O}$], Chromium Nitrate – [$\text{Cr}(\text{NO}_3)_3 \cdot 9\text{H}_2\text{O}$], Citric acid - ($\text{C}_6\text{H}_8\text{O}_7 \cdot \text{H}_2\text{O}$) used as starting materials for the synthesis.

2.2 Synthesis of nanoparticles

Metal nitrates in required proportions were dissolved in a minimum quantity of distilled water and mixed together. Aqueous solution of Citric acid was then added to the mixed metal nitrate solution (with and without Samarium nitrate). Ammonia solution was then added with constant stirring by maintaining the neutral pH

(7.0). The solutions were heated at 90°C under continuously stirring to remove the excess of the solvent. By raising the temperature upto 200°C lead the ignition of gel. The dried gel burnt completely in a self-propagating combustion manner to form powder like substance. The burnt powder was ground in Agate Mortar and Pestle to get a fine Ferrite powder. Finally the burnt powder was calcined in air at 700°C temperature for 2 hours and cooled to room temperature.

2.3 Characterization

2.3.1 X-ray Diffraction

The XRD analysis on the prepared samples was made using a SCINTAG X'TRA AA85516 (Thermo ARL) X-ray diffractometer equipped with a Peltier cooled Si solid detector. Monochromatized $\text{Cu K}\alpha$ ($\lambda = 1.5405 \text{ \AA}$) was used as the radiation. Diffraction patterns were collected at 45 kV–40 mA, at 0.02°C step and count time of 0.400 sec over a range of 10.00–80.0 (2θ), at a step scan rate of 3.00 min^{-1} and the crystallite size (D) is calculated from X-ray line broadening of the (311) diffraction peak using the well-known Debye-Scherrer's formula⁷:

$$D = \frac{0.9\lambda}{\beta \cos\theta} \dots \dots \dots (1)$$

where β is the full-width at half-maxima of the strongest intensity diffraction peak (311), λ the wavelength of the radiation, and θ the angle of the strongest characteristic peak.

X-ray density (ρ_x) was calculated using the following equation:

$$\rho_x = \frac{8M}{Na^3} \dots \dots \dots (2)$$

where M is the molecular weight (gm), N Avogadro's number (per mol) and a the lattice parameter in angstrom.

The value of lattice parameter a determined from the high intense peak (311) of XRD pattern using the following equation⁸ and values are given in Table 1.

$$a = \frac{d_{hkl}}{(\sqrt{h^2+k^2+l^2})} \dots \dots \dots (3)$$

where a is lattice constant d_{hkl} is inter-planar distance for hkl plane.

2.3.2 FTIR Spectroscopic Analysis

Nanoferrites chemical composition is examined using Fourier Transform Infrared spectroscopy (FTIR). The sample discs were

prepared by mixing of 1 mg of powdered carbon with 500 mg of KBr (Merck-spectroscopy quality) in an agate mortar, then pressing the resulting mixture successively under a pressure of 5 tones/cm² for about 5 min., and at 10 tones/cm² for 5 min., under vacuum. The spectra were measured from 4000 to 400 cm⁻¹ on a JASCO-FTIR-5300 model.

2.3.3 SEM-EDX analysis

The surfaces of the powder carbonaceous materials have been stubbed using the double-sided adhesive carbon tape. Samples are coated with the help of platinum coater [JOEL Auto fine coater model, JFC -1600 auto fine coater, Coating time is 120 sec with 20mA] and deposited with a thin layer of platinum on the sample. The microphotographs of these samples were recorded using SEM JEOL model, JSM-5600 equipped with EDX Analyzer, an accelerating voltage of 5 kV, at high vacuum mode. The maximum magnification possible in the equipment is 3,00,000 times with a resolution of 3 nm, typically setting at various magnifications for all the samples of study.

2.3.4 TEM analysis

The ferrite sample was first sonicated (Vibronics VS 80) for 5 minutes. Ferrites were loaded on carbon coated copper grids, and solvent was allowed to evaporate under Infra light for 30 minutes. TEM measurements were performed on Phillips model CM 20 instrument, operated at an accelerating voltage at 200 kV.

Hysteresis Tracer was employed to study the magnetic properties of the samples in the field of 10 kOe at room temperature.

3.0 RESULTS AND DISCUSSION

3.1 XRD studies: The typical X-ray diffraction patterns of Sm_x Mn_{0.3} Cr_{0.3} Fe_{2-x}O₄ (where X=0.0, 0.2, 0.4) Nano ferrites and those annealed at 700°C are shown in Figure 1. The crystalline phase and the

peaks identification done by comparing the 'd' spacing with that of JCPDS data⁹ of Mn Fe₂O₄ and Cr Fe₂O₄. The major lattice planes (220), (311), (222) (400), (422), (511), (440), (533), (622) and (444) in figure 1 confirm the formation of single phase with a face centred cubic (fcc) spinel structure. This implies that the Sm³⁺ ions have been completely dissolved into the spinel lattice of Mn-Cr ferrite.

The average crystallite size for the prepared samples has been calculated from the line broadening of the most intense peak (311) plane of the spinel structures using the Scherer equation⁸. It is observed that the particle size decreases as increasing the concentration of Sm³⁺ cation concentration, which is also confirmed by the TEM studies.

The Samarium ions have a tendency of replacing the Fe³⁺ cations in the octahedral sites which can be concluded from the invariance of the lattice constant values for the various concentrations of Sm³⁺ ions. The peaks become broader as the Sm³⁺ ion content increases thereby indicating a regular decrease in the particle size which is marked from the values of crystallite sizes that are tabulated in Table 1 and similar results were also found in previous studies¹⁰.

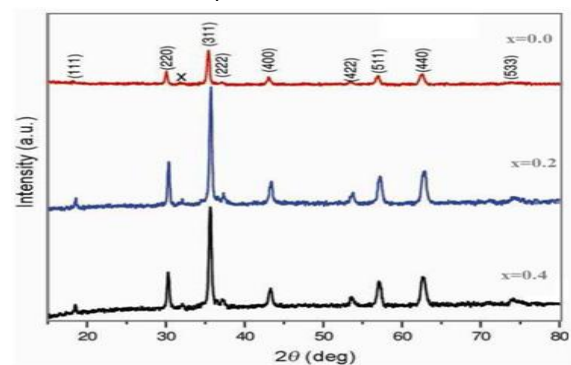


Figure 1: X-ray diffraction patterns of Sm_x Mn_{0.3} Cr_{0.3} Fe_{2-x}O₄ Nano ferrites

Table 1: Crystal & Magnetic Parameters of Mn-Cr Ferrites for various concentrations of Sm³⁺ ion

Concentration of Sm ³⁺ ion	Crystallite size (nm)	Lattice constant (Å)	X-ray density (g cm ⁻³)	Magnetization (emu/g)	Coercivity (Oe)	Retentivity (emu)
0.0	20.21	8.6425	6.56	22.939	1472.47	18.12
0.2	18.97	8.6772	7.33	21.681	1810.61	17.06
0.4	19.06	8.6079	7.37	19.933	1766.80	16.94

3.2 FTIR studies: Fourier transform infrared (FTIR) studies were carried out to study the metal-oxygen bonding in the prepared Nano ferrite samples. FTIR spectra of the prepared ferrite nano particles measured in the frequency range of 700cm^{-1} to 400cm^{-1} are shown in figure 2. The formation of the spinel structure of Mn-Sm-Cr ferrite system is supported by FT-IR analysis. In the range of wavenumber 700 to 400cm^{-1} , there is two prominent absorption bands ν_1 and ν_2 corresponding to the stretching vibration of the tetrahedral and octahedral sites around 550 to 556cm^{-1} respectively were observed (table 2). These absorption bands denote distinguishing features of spinel ferrites in single phase. The difference between ν_1 and ν_2 is due to the changes in bond length of Fe-O at the Octahedral and Tetrahedral sites. From the table it is clear that the high frequency band (ν_1) lies in the range of 551 to 557cm^{-1} , while a significant change was observed in ν_2 band by Sm^{3+} substitution corresponding to octahedral site. It is observed that the ν_2 band (octahedral site) lies in the range of 460 and 467cm^{-1} and has a subsidiary band ν_3 in the range of 433 and 428cm^{-1} , for two samples except for pure Mn-Cr ferrite. This may be due to Jahn-Teller distortion produced by doping Sm^{3+} which has been reported earlier by Mamilla Lakshmi et al¹¹. It can be seen from figure 2 that the values shift to lower-frequency side with increasing Sm^{3+} content. Also a slight broadening of the absorption band is also noticed with increase in samarium concentration. This may be attributed to the substitution of Fe^{3+} ions by Sm^{3+} ions¹².

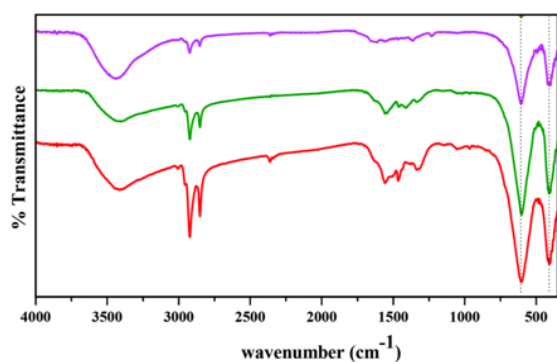


Figure 2: FTIR spectra of $\text{Sm}_x\text{Mn}_{0.3}\text{Cr}_{0.3}\text{Fe}_{2-x}\text{O}_4$ Nano ferrites

Table 2: FTIR parameters of $\text{Sm}_x\text{Mn}_{0.3}\text{Cr}_{0.3}\text{Fe}_{2-x}\text{O}_4$ Nano ferrites

Ferrite Composition	$\nu_1(\text{cm}^{-1})$	$\nu_2(\text{cm}^{-1})$	$\nu_3(\text{cm}^{-1})$
$\text{Sm}_0\text{Mn}_{0.3}\text{Cr}_{0.3}\text{Fe}_2\text{O}_4$	552.7	433.6	not identified
$\text{Sm}_{0.2}\text{Mn}_{0.3}\text{Cr}_{0.3}\text{Fe}_{1.8}\text{O}_4$	554.6	467.3	429.0
$\text{Sm}_{0.4}\text{Mn}_{0.3}\text{Cr}_{0.3}\text{Fe}_{1.6}\text{O}_4$	556.6	461.9	432.9

3.3 SEM – EDX analysis: The surface morphology of the prepared nano ferrites studied using scanning electron microscope (SEM) and corresponding results were shown figure 3(a-c). It was clear from electron micrographs that the material basically consists of some irregularly cubic or rod like particles in pure Mn-Cr ferrite (Figure 3(a)) and agglomeration of these particles increases with the increase in Sm^{3+} ions concentration. The appearance of these agglomerates may be attributed to sintering process as a result of chemical reaction. Magnetic forces or even relatively weak Vander Waals bonds might be responsible to hold these agglomerates together. Well-crystallized dense grains of irregular shapes were observed for Samarium compositions with the presence of small micro pores. The continuous decrease in grain size with Sm^{3+} substitution may be due to the fact that Samarium ions have large ionic radii than that of Iron (0.64Å) and, therefore, show limited solubility in spinel lattice and prevent grain growth resulting in decrease in grain size¹³.

The composition of the sample was determined by the EDS and the pattern obtained is shown in Figure 3(a-c) (right side). The specimen shows presence of Mn, Fe, Cr, O and Sm (except in figure 3a), in the sample and did not contain any other impurities. This indicates the purity of the prepared sample.

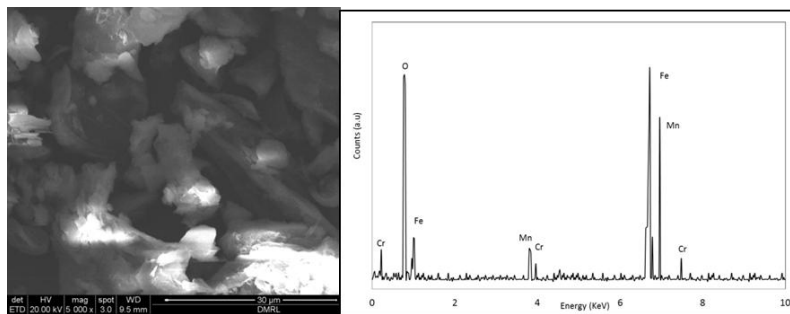


Figure 3a: SEM-EDX spectra of $\text{Sm}_0 \text{Mn}_{0.3} \text{Cr}_{0.3} \text{Fe}_2 \text{O}_4$

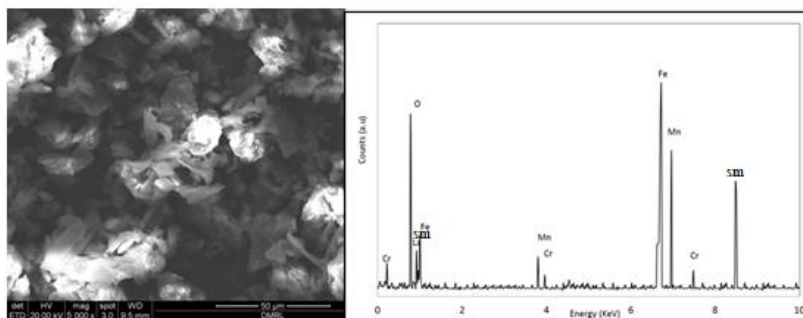


Figure 3b: SEM-EDX spectra of $\text{Sm}_{0.2} \text{Mn}_{0.3} \text{Cr}_{0.3} \text{Fe}_{1.8} \text{O}_4$

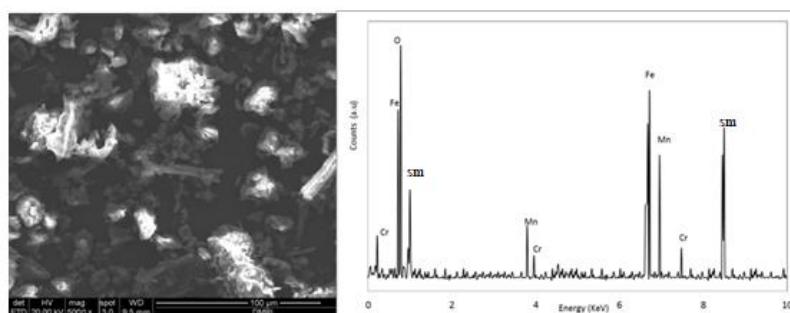


Figure 3c: SEM-EDX spectra of $\text{Sm}_{0.4} \text{Mn}_{0.3} \text{Cr}_{0.3} \text{Fe}_{1.6} \text{O}_4$

3.4 TEM analysis: The TEM micrographs of three nano ferrite samples exhibit highly agglomerated particles due to the interfacial surface tension as reported in literature. It can be seen that most of the nanoparticles appear with almost spherical shape (and are slightly agglomerated (Figure 4a-4c). The average particle size obtained from TEM analysis is decreased by increasing the concentration of Samarium ion like 19.18 nm ($\text{Sm}=0.0$), 18.72 nm ($\text{Sm}=0.25$) and 18.545 ($\text{Sm} = 5.0$). The similar pattern also supported by XRD studies.

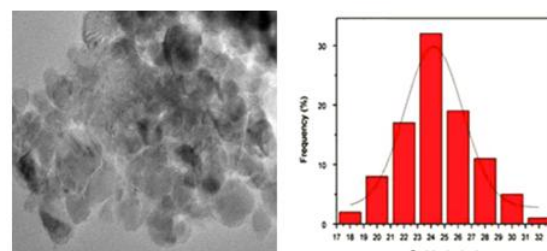


Figure 4a: TEM images (left) of $\text{Sm}_0 \text{Mn}_{0.3} \text{Cr}_{0.3} \text{Fe}_2 \text{O}_4$ and particle size distribution (right)

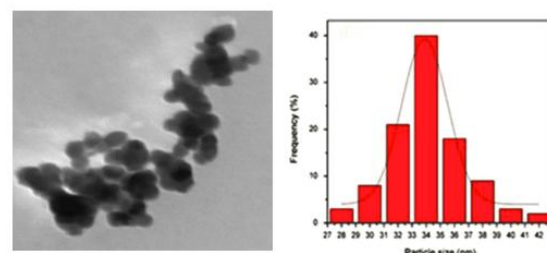


Figure 4b: TEM images (left) of $\text{Sm}_{0.2} \text{Mn}_{0.3} \text{Cr}_{0.3} \text{Fe}_{1.8} \text{O}_4$ and particle size distribution (right)

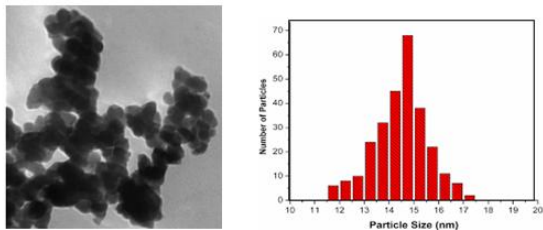


Figure 4c: TEM images (left) of $\text{Sm}_{0.4}\text{Mn}_{0.3}\text{Cr}_{0.3}\text{Fe}_{1.6}\text{O}_4$ and particle size distribution (right)

3.5 Magnetic properties: The magnetic parameters of prepared nano ferrite samples were calculated by using a vibrating sample magnetometer (VSM) in the range 5000 Oe, where the samples displayed the magnetic behaviour. The hysteresis loops (figure 5) were plotted from the VSM measurements, from which the saturation magnetisation values for the different compositions $\text{Sm}_x\text{Mn}_{0.3}\text{Cr}_{0.3}\text{Fe}_{2-x}\text{O}_4$ ($x=0.0, 0.2$ and 0.4) were calculated and represented graphically in Figure 5 and tabulated in table 1. The variation of saturation magnetisation with composition is as shown the figure 5 and figure 6, it was evident from the hysteresis loops that the sample does not saturate completely for values ($x= 0.0, 0.2, 0.4$). From the result it is clear that the saturation magnetization decreases with the substitution of Samarium. This decrease can be explained based on the site occupancy of the cations and also the modification in the exchange effects caused by substituting Samarium. The Fe^{3+} ions occupying the 'B' sites in the inverse spinel lattice are the main contributors of the magnetic properties. Sm^{3+} has no unpaired electrons and is paramagnetic in nature. There is a significant decrease in the coercivity with the substitution of Sm^{3+} . This theory states that the factors such as microstrain, magneto crystalline anisotropy, magnetic particle morphology, magnetic domain size and size distribution influence the coercivity¹¹.

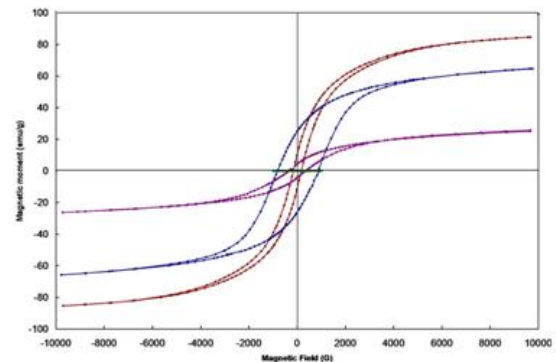


Figure 5: Hysteresis loops of Manganese Chromium ferrite for various Sm^{3+} concentrations

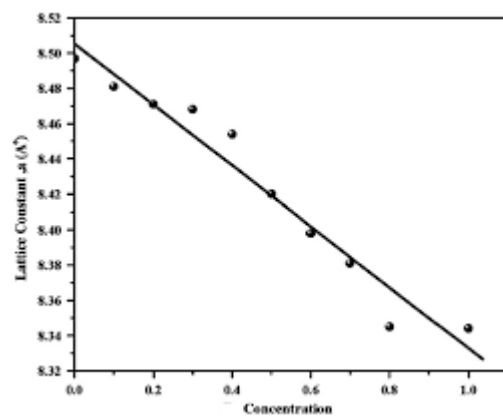


Figure 6: Plot of Magnetization Vs Concentration

4.0 Conclusion

The experimental investigation shows how properties of spinel Samarium substituted Mn-Cr ferrites are affected by doping of Samarium. The investigated samples developed through the sol-gel method and performed for structural and magnetic measurements on sintering temperature at 700°C . From the entire study we concluded that:

- X-ray diffraction results showed the presence of all characteristic reflections (220), (311), (222), (400), (422), (511), (440), (222), (533), (622), and (444) which confirmed the formation of single phase, cubic spinel structure. Lattice constant and crystallite size decrease with Sm^{3+} substitution.
- The FTIR spectrum of the synthesized Nano crystal confirms the formation of the spinel structure with strong Metal oxygen bond.
- SEM images show the fused grain nature with inter granular diffusion in $\text{Sm}_x\text{Mn}_{0.3}\text{Cr}_{0.3}\text{Fe}_{2-x}\text{O}_4$ ($x=0.0, 0.2$ and 0.4) Nano ferrites.
- For three samples, 'S' like shape hysteresis curve was observed. Magnetic parameters decrease with

increasing Sm^{3+} substitution. The gradual increase in the Sm content brought about a decrease in the crystallite size followed by a decrease in the saturation magnetisation

5.0 References

- 1 V. G. Harris, A. Geiler, Y. J. Chen, S, et al., Recent Advances in Processing and Applications of Microwave Ferrites, *J. Magn. Mater.*, 321, 2035 (2009).
- 2 S. Suder, B.K. Srivastava, A. Krisnamurty, *Ind. J. Pure Appl. Phys.* 42 (2004) 366.
- 3 S. Yáñez-Vilar, M. Sánchez-Andújar, C. Gómez-Aguirre, J. Mira, M. A. Señaís-Rodríguez, and S. Castro-García, "A simple solvothermal synthesis of MFe_2O_4 (M = Mn, Co and Ni) nanoparticles," *Journal of Solid State Chemistry*, vol. 182, no. 10, pp. 2685–2690, 2009
- 4 D. Zhang, X. Zhang, X. Ni, J. Song, and H. Zheng, "Low-temperature fabrication of MnFe_2O_4 octahedrons: magnetic and electrochemical properties," *Chemical Physics Letters*, vol. 426, no. 1–3, pp. 120–123, 2006.
- 5 Q. Zhang, M. Zhu, Q. Zhang, Y. Li, and H. Wang, "Fabrication and magnetic property analysis of monodisperse manganese-zinc ferrite nanospheres," *Journal of Magnetism and Magnetic Materials*, vol. 321, no. 19, pp. 3203–3206, 2009
- 6 Gagan Kumar, Jyoti Shah, R. K. Kotnala, Pooja Dhiman, Ritu Rani, Virender Pratap Singh, Godawari Garg, Sagar E. Shirsath, Khalid M. Batoor, M. Singh. Self-ignited synthesis of Mg-Gd-Mn nanoferrites and impact of cation distribution on the dielectric properties. *Ceram. Inter.* 2014, 40, 14509-14516
- 7 P. Scherrer, *Göttinger Nachrichten Gesell.*, Vol. 2, 1918, p 98
- 8 Krishna, K.R., Ravinder, D., Kumar, K.V. and Lincon, C.A. (2012) Synthesis, XRD & SEM Studies of Zinc Substitution in Nickel Ferrites by Citrate Gel Technique. *World Journal of Condensed Matter Physics*, 2, 153-159
- 9 M. Raghasudha, D. Ravinder, and P. Veerasomaiah, "Effect of Cr Substitution on Magnetic Properties of Mg Nanoferrites Synthesized by Citrate-Gel Auto Combustion Method," *Journal of Chemistry*, vol. 2013, Article ID 804042, 6 pages, 2013. doi:10.1155/2013/804042
- 10 Sopan M. Rathod, Sarang S. Bhosale, Pratik Kumar K. Zagade, Datta B. Pawar, Ashok B. Shinde, Synthesis and Characterization of La^{3+} Doped Ni Nano Ferrite by Sol-Gel Method, *BIONANO FRONTIER*, Vol. 8 (3) December 2015
- 11 Lakshmi, M. , Kumar, K. and Thyagarajan, K. (2016) Structural and Magnetic Properties of Cr-Co Nanoferrite Particles. *Advances in Nanoparticles*, 5, 103-113.
- 12 B. P. Jacob, S. Thankachan, S. Xavier, and E. M. Mohammed, "Effect of Gd^{3+} doping on the structural and magnetic properties of nanocrystalline Ni–Cd mixed ferrite," *Physica Scripta*, vol. 84, no. 4, Article ID 045702, 2011.
- 13 C. Kittel, *Introduction a La Physique de L'etat Solide*, Dunod, Paris, France, 1958.